Applied Surface Science 271 (2013) 60–69

Contents lists available at SciVerse ScienceDirect

Applied Surface Science

journal homepage: www.elsevier.com/locate/apsusc

Association of poly(*N*-isopropylacrylamide) containing nucleobase multiple hydrogen bonding of adenine for DNA recognition

Hsiu-Wen Yang[a], Jem-Kun Chen[a,*], Chih-Chia Cheng[b], Shiao-Wei Kuo[b]

[a] Department of Materials Science and Engineering, National Taiwan University of Science and Technology, 43, Sec 4, Keelung Road, Taipei, 106, Taiwan, ROC
[b] Department of Applied Chemistry, National Chiao Tung University, 1001 University Road, Hsinchu, 300, Taiwan, ROC

ARTICLE INFO

Article history:
Received 2 November 2012
Received in revised form 11 January 2013
Accepted 12 January 2013
Available online 29 January 2013

Keywords:
Supramolecule
Poly(*N*-isopropylacrylamide)
Adenine
DNA recognition

ABSTRACT

In this study we used the poly(*N*-isopropylacrylamide) (PNIPAAm) as a medium to generate PNIPAAm–adenine supramolecular complexes. A nucleobase-like hydrogen bonding (NLHB) between PNIPAAm and adenine was found that changed the morphology, crystalline structure, and temperature responsiveness of PNIPAAm microgels relatively to the adenine concentrations. With increasing the adenine concentration, the PNIPAAm–adenine supramolecular complexes gradually altered their morphologies from microgel particles to thin film structures and suppressed the thermodynamical coil-to-globule transition of PNIPAAm because of the NLHB existed between the PNIPAAm amide and ester groups and the adenine amide groups (C═O···H—N and N—H···N—R), verified by FTIR spectral analysis. NLHB was also diverse and extensive upon increasing the temperature; therefore, the thermoresponsive behavior of the complexes was altered with the NLBH intensity, evaluated by the inter-association equilibrium constant (K_a) above and below their LCST. Therefore, PNIPAAm can be as a medium to recognize adenine in various concentrations, which could potentially be applied in DNA recognition.

1. Introduction

Intelligent polymers, which have the ability to respond to external stimuli (e.g., small changes in temperature and pH), have attracted great interest for several biomedical and bioengineering applications, including protein–ligand recognition [1], capture/release for DNA extraction [2,3], the development of artificial organs [4], and DNA diagnosis device [5,6]. Stimuli-responsive polymers are defined as polymers that undergo relatively large and abrupt, physical or chemical changes in response to small external changes in the environmental conditions [7]. Polymer precipitation in solution on raising the temperature often occurs in aqueous systems and results from the balance of intermolecular forces between the polymer and the solvent as well as between polymers [8]. One of the unique properties of temperature-responsive polymers is the presence of a lower critical solution temperature (LCST). Critical solution temperature is the temperature at which the phase of polymer and solution (or the other polymer) is discontinuously changed according to their composition [9,10].

As mentioned previously, polymers based on NIPAAm are part of a group of polymers that exhibit an LCST. Poly(*N*-isopropylacrylamide) (PNIPAAm) and its copolymers belong to the most intensively investigated thermoreversible systems. Recent developments on PNIPAAm-based hydrogels include their use for drug delivery [11] cell encapsulation and delivery [12] and cell culture surfaces [13]. The LCST for PNIPAAm occurs around 32 °C for PNIPAAm chains, depending on the polymer's molecular structure. Below the LCST, PNIPAAm assumes a flexible, extended in a random coil configuration through intermolecular hydrogen-bonding (HB) [14]. Above the LCST, it becomes hydrophobic and the polymer chains seem to collapse prior to aggregation in globular structures through intramolecular HB [15]. So, there is a need to develop non-toxic, biodegradable hydrogels for the biomedical applications without losing their smart properties, such as temperature sensitivity [16]. In biological systems, complementary multiple HB interactions are paramount for stability; for example, in DNA and RNA, molecular recognition occurs primarily through multiple adenine–thymine (A–T), adenine–uracil (A–U), and guanine–cytosine (G–C) base pairs [17]. Adenine, a purine nucleobase, is an important naturally occurring nitrogen heterocycle present in nucleic acids DNA and RNA. Nucleobases have recently been recognized as versatile and flexible supramolecular building blocks. Their propensity to self-assemble into larger aggregates through HB interactions or metal coordination has led to a plethora of supramolecular structures, often with intriguing architectures. More recently, increasing numbers of mechanical approaches are emerging in which a nucleobase interacts with a complementary small organic molecule through DNA base pair oscillations [18]. Adenine and its derivatives contain both HB acceptor and donor functionalities, as well as protonatable nitrogens [19].

* Corresponding author. Tel.: +886 2 27376523; fax: +886 2 27376544.
E-mail address: jkchen@mail.ntust.edu.tw (J.-K. Chen).

0169-4332/$ – see front matter © 2013 Elsevier B.V. All rights reserved.
http://dx.doi.org/10.1016/j.apsusc.2013.01.074

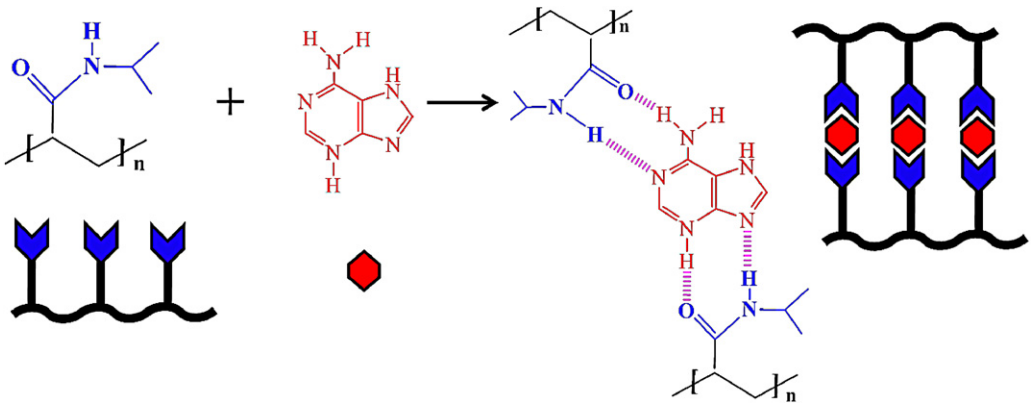

Scheme 1. Representation of the supramolecular structure formed from the complexation of PNIPAAm and adenine through NLHB interactions.

Although many synthetic polymers have been functionalized to feature complementary nucleobases adenine and thymine [20], few reports describe supramolecules formed through the incorporation of adenine into hydrogels. In this paper, we describe PNIPAAm complexes formed with adenine moieties through their specific interaction, so called nucleobase-like hydrogen bonding (NLHB), between the amide and ester groups of PNIPAAm side chains and the amide groups of adenine (C=O···H–N and N–H···N–R) (Scheme 1)—that assemble to form sheet structure. These sheet architectures formed using adenine as an agent to crosslink the side chains of PNIPAAm promise candidates for adenine detection. This method for the adenine detection in various concentrations with PNIPAAm would be cheaper and less time-consuming. An additional advantage of assembling through HB is that understanding the biocomplementary interactions between PNIPAAm and adenine through NLHB at multiple sites [21].

2. Experimental

2.1. Materials

N-isopropylacrylamide (NIPAAm), 2-bromine methyl propionate (BP), copper(I) bromide, copper(II) bromide, triethylamine (TA), and 1,1,4,7,7-pentamethyldiethylenetriamine (PMDETA) were purchased from Acros Organics. NIPAAm, PMDETA, AS, and BB were purified through vacuum distillation prior to use. Adenine was purchased from Sigma–Aldrich. All other chemicals and solvents were of reagent grade and purchased from Aldrich Chemical. PNIPAM was synthesized by the atom transfer radical polymerization (ATRP) of NIPAAM using BP as the initiator and CuBr as the catalyst. TA was used as the ligand in this system [22]. The polymerization of NIPAAm monomer with 0.16 g CuBr and 0.38 g TA were added into the reaction flask and 10 mL toluene was then added. The sample was first stirred and then degassed by purging with nitrogen. Subsequently, 10 g NIPAAM and 0.15 g BP were added into the flask and degassed with nitrogen. Polymerization was performed at 40 °C for 24 h and monomer conversion was above 70%. PNIPAAM was purified by passing through an Al_2O_3 column to remove the CuBr catalyst followed by a precipitation in a toluene/n-hexane mixture (3:7, v:v). The precipitate of PNIPAAM was then filtered under vacuum and dried in a vacuum oven at room temperature. 1H NMR ($CDCl_3$, ppm): 7.03 [1H, NH–CH], 1.97 [2H, CH_2–CH], 3.83 [1H, NH–CH], 1.05–1.62 [6H, CH–CH_3–CH_3].[23] GPC: M_n = 27,000 with M_w/M_n = 1.26. Complexation experiments between adenine and PNIPAAm were performed in DMSO at PNIPAAm-to-adenine weight ratios for the various complex preparations in DMSO were 80:20, 50:50, and 20:80 (herein denoted P80A20, P50A50, and P20A80, respectively). Dispersions of PNIPAAm microgels were added dropwise to adenine solutions to give a final PNIPAAm concentration of 1 mg/mL in the solutions, which were stirred for 30 min at room temperature. The concentration of the complexes formed from PNIPAAm and adenine in DMSO solution was controlled at 10 wt%; the solvent was then were dried in a vacuum chamber at room temperature for 2 days before the PNIPAAm–adenine complex films were lyophilized for 3 h prior to further analysis.

3. Thermoresponsive behavior of the complexes

The thermal properties and phase transitions of the complexes were investigated through differential scanning calorimetry (DSC) using a 910 DSC-9000 controller (DuPont) operated at a scan rate of 10 °C/min in the temperature range 30–200 °C under a N_2 atmosphere. The sample (ca. 5–10 mg) was weighed and sealed in an aluminum pan. It was then quickly cooled to room temperature from the first scan and then scanned between 30 and 220 °C at a scan rate of 5 °C/min. The glass transition temperature (T_g) was taken as the midpoint of the heat capacity transition between the upper and lower points of deviation from the extrapolated glass and liquid lines. The obtained complex colloidal solutions were very stable and did not exhibit any signs of decomposition or aggregation over a period of several weeks. The turbidity (cloud point temperature (CPT)) of PNIPAAm and PNIPAAm–adenine aqueous dispersions was measured at a concentration of 0.1 wt% using a Varian-Cary 100 UV–vis spectrophotometer, equipped with a water-jacketed quartz cell holder coupled to a temperature-controlled circulating bath. The transmittance of the complex solutions was measured at 550 nm in the temperature range from 24 °C to 50 °C using a thermo stated cell. The temperature was increased at a rate of 0.2 °C/min. The sample was allowed to equilibrate for 10 min at each temperature. The increase in turbidity with increasing temperature for both PNIPAAm itself and the PNIPAAm–adenine complexes was a result of a volume phase transition. The LCST for the thermoresponsive samples was calculated from the inflection point of the normalized absorbance-to-temperature curve. The hydrodynamic diameters of the assemblies were measured through dynamic light scattering (DLS) using a Zetasizer Nano S90 instrument (Malvern Instruments, UK) equipped with a He–Ne laser operated at 25–50 °C.

4. Morphological analyses of PNIPAAm–adenine complexes

PNIPAAm–adenine aqueous solutions were dip-coated onto glass without specific flatting. The lyophilized complexes were observed through field-emission scanning electron microscopy (FE-SEM) using a JEOL JSM 6500F instrument operated at 15 kV.

Glancing-angle X-ray diffraction (XRD) measurements (angle of incidence [x] = 2) were performed at room temperature in the parallel beam geometry with Cu Kα radiation (k = 15.418 nm) and thin film equipment. The registered diffraction angle (2θ) ranged from 20° to 95° with a step size ($\Delta 2\theta$) of 0.05° and a measuring time of 40 s/step. Static water contact angles (SWCAs) were measured by a contact angle (CA) meter (Sindatek Instruments) at temperatures of 25 and 45 °C [24]. The specimens for examination under an electron microscope were prepared through evaporation of one or two drops of a toluene solution of the complexes onto holey carbon films supported on standard Cu grids. Phase contrast images of the complexes were obtained through transmission electron microscopy (TEM) using a Philips Tecnai G2 F20 instrument operated at an accelerating voltage of 200 kV (point resolution: 0.248 nm).

5. Assessment of NLHB by FTIR spectra and association constants

The HBs between the PNIPAAm and adenine units in the complexes were analyzed using Fourier transform infrared (FTIR) spectroscopy to assess the reversibility of complexation and decomplexation and its effects on the thermoresponsive behavior of PNIPAAm. FTIR spectroscopy can provide information relating to the specific interactions between polymers, both qualitatively and quantitatively. FTIR spectra of samples under N_2 were recorded using a Nicolet AVATAR 32 apparatus at a spectral resolution of 1 cm^{-1}. A total of 256 scans were accumulated for signal-averaging of each measurement to ensure a high signal-to-noise ratio with a resolution of 1 cm^{-1}. Variable-temperature FTIR spectra were recorded between 30 and 180 °C; each temperature point was maintained for 30 min to collect the IR spectrum and then the temperature was increased or decreased by 30 °C manually.

Deter UV–vis absorption spectra in aqueous solution by using a quartz cell having 1.0 cm pathway were all recorded on a computer-controlled Varian-Cary 100 UV–vis spectrophotometer. PNIPAAm were solved in 30 mL of adenine solution with various concentrations (concentration range from 5×10^{-5} mol/L to 5×10^{-4} mol/L), each holding the same amount of PNIPAAm. Afterward, gel samples were left to swell/deswell sufficiently until an equilibrium state while thermostated in a water bath at a given temperature. Variations thus occurred in UV absorbance of adenine solution with different concentrations were monitored on a UV–vis spectrophotometer with wavelength fixed at 260 nm. Then, association constant K_a (L/mol) could be readily obtained from a linearized Benesi-Hildebrand equation. The process mentioned above was repeated at each given temperature to determine the temperature dependence of K_a. The association constant (K_a) of the complex of PNIPAAm and adenine is calculated using the Benesi-Hildebrand equation [25]. Benesi-Hildebrand equation was employed to quantitatively describe the interaction between PNIPAAm and adenine at different temperatures. For the binary PNPAAm-adenine complexes, the following equilibrium should be considered Eq. (1), and the association constant K_a is given by Eq. (2).

$$\text{adenine} + \text{PNIPAAm} \leftrightarrow \text{adenine} - \text{PNIPAAm} \quad (1)$$

$$K_a = \frac{[\text{adenine} - \text{PNIPAAm}]}{[\text{adenine}]/[\text{PNIPAAm}]} \quad (2)$$

The binding constants of PNIPAAm and adenine can be quantitatively determined using the Benesi-Hildebrand equation in the following modified form [26].

$$\frac{1}{\Delta A} = \frac{1}{K_a \Delta A_{max}} \times \frac{1}{[\text{PNIPAAm}]} + \frac{1}{\Delta A_{\max}} \quad (3)$$

where $\Delta A_{\max}$ is the maximum change of the absorbance area of the adenine NH protons corresponding to complete formation of the associated complex. The slope of the double reciprocal plot is $1/K_a \Delta A_{\max}$, and the intercept is $1/\Delta A_{\max}$. The K_a was calculated from the slope of the plot, which is consistent with K_a values reported earlier for adenine base pair recognition.

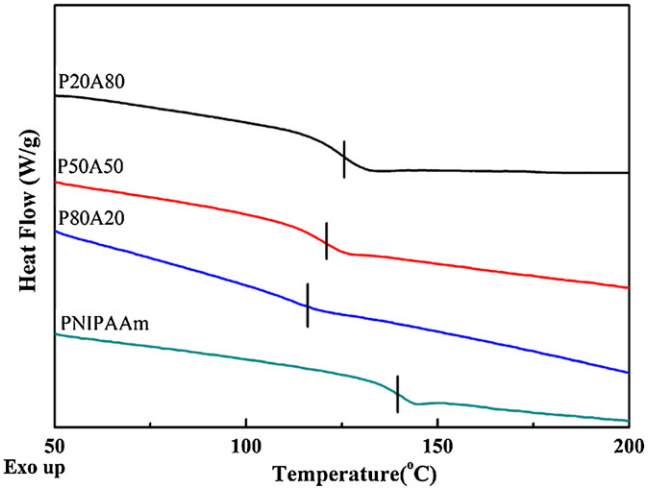

Fig. 1. Conventional second-run DSC thermograms of PNIPAAm and the PNIPAAm–adenine complexes P80A20, P50A50, and P20A80.

6. Results and discussion

6.1. Thermoresponsive behavior of the PNIPAAm–adenine complexes

Fig. 1 displays conventional second-run DSC thermograms of PNIPAAm–adenine complexes for pure PNIPAAm, P80A20, P50A50 and P20A80, respectively. Introduction of the adenine in the PNIPAAm, the original HBs, provided by the amide groups interacting the interpolymer and intrapolymer segments, in the PNIPAAm were suppressed, resulting in the decrease of T_g for P80A20. With increasing the adenine above 20 wt%, the local motion of polymer segments was retarded initially by the adenine because of high tendency to attract the amide hydrogen atoms and interfere with the HBs between the amide groups of PNIPAAm. This competition presumably rearranged the PNIPAAm chain segments to form a different molecular structure, so-called NLHB. The increased NLHB gradually stabilized the supermolecular structure of the PNIPAAm–adenine complexes (Scheme 1), increasing the value of T_g from 112.4 °C for P80A20 to 128.6 °C for P20A80 [27].

Although the cloud point, measured at the onset of the turbidity upon increasing the temperature, may be an overestimation of the LCST, it still provides an acceptable estimation of the LCST within a stipulated temperature scanning rate if the aggregation kinetics are sufficiently rapid. Fig. 2a displays the changes in turbidity for pure PNIPAAm and the PNIPAAm–adenine complexes P80A20, P50A50, and P20A80 as a function of temperature. LCSTs of the complex aqueous solutions increased linearly upon increasing the adenine content (Fig. 2b), with values of 34, 36, and 39 °C for P80A20, P50A50, and P20A80, respectively [28]. Note that transmittances of P50A50 and P20A80 approached only approximately 55% during their phase transitions; such partial miscibility indicates that the complexes in aqueous solution above the LCST did not undergo complete coil-to-globule transitions with water, due to the presence of NLHB. Furthermore, the degrees of NLHB in both P50A50 and P20A80 may have approached saturation because of their similar miscibilities in aqueous solutions. The photographic images in Fig. 2c of the complexes all clearly

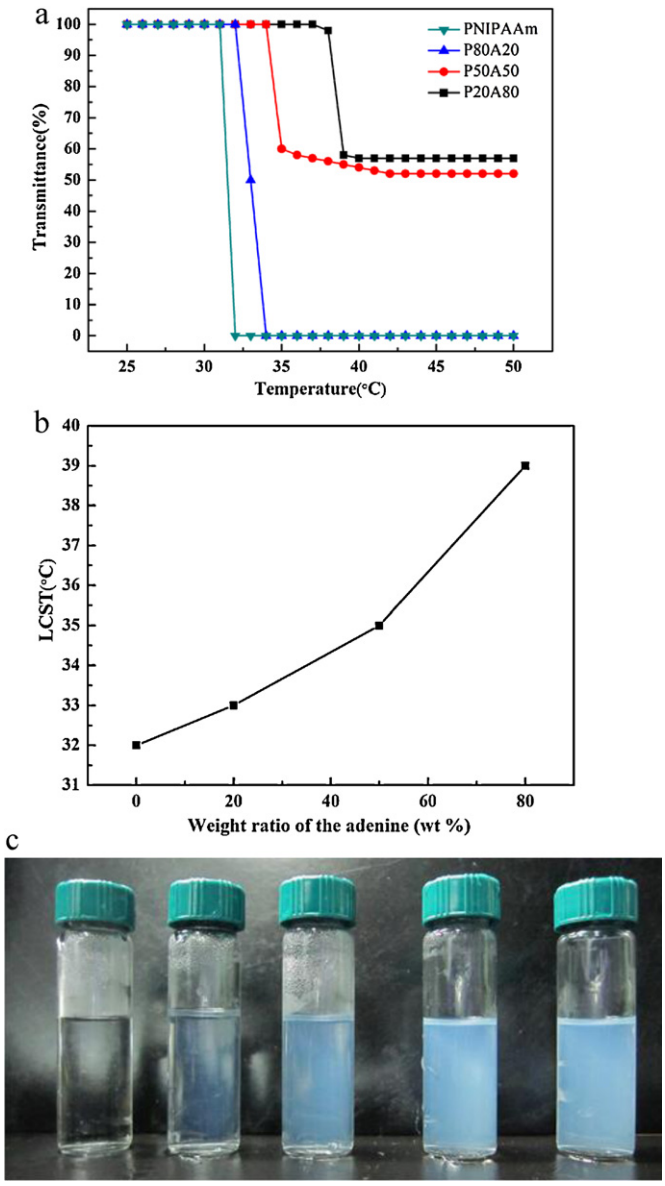

Fig. 2. (a) Turbidimetry analysis of PNIPAAm and the PNIPAAm–adenine complexes P80A20, P50A50, and P20A80 in aqueous solution. The data were obtained upon heating from 25 °C up to a temperature at which a transmittance plateau was clearly defined. A similar profile was obtained upon cooling, with no significant hysteresis. (b) LCSTs of these complexes, recorded as a function of the adenine content. (c) Photographs of aqueous solutions at 45 °C of (from left to right) pure adenine, P20A80, P50A50, P80A20, and pure PNIPAAm.

exhibit turbidity changes in their aqueous solutions at 45 °C. This predominant NLHB model partially suppressed the coil-to-globule transition, generating semi-miscibility above their LCSTs [29]. In addition, we used dynamic light scattering (DLS) to characterize the supramolecular structures in the complex aqueous solutions and to verify the changes in miscibility and the semi-transparent properties of the complexes above their LCSTs; we determined particle sizes of the complexes with increasing the temperature of their solutions [30]. Fig. 3 plots hydrodynamic radii of the complexes with respect to temperatures of the aqueous solution. Above their LCSTs, all of the samples including PNIPAAm, P80A20, P50A50, and P20A80 possessed sizes close to 220 nm, suggesting that the semi-miscibility phenomena occurred without changing the hydrodynamic radii of the complexes in aqueous solution.

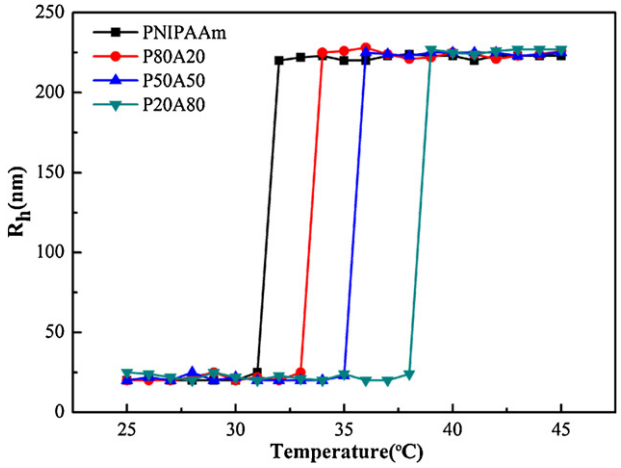

Fig. 3. Hydrodynamic radii of pure PNIPAAm and the PNIPAAm–adenine complexes P80A20, P50A50, and P20A80 at various temperatures.

7. Surface morphology and characterization of the PNIPAAm–adenine complexes

Fig. 4 reveals that the surfaces of pure PNIPAAm and the complexes P80A20, P50A50, and P20A80 all exhibited thermally responsive switching between their hydrophilic and hydrophobic states below and above their LCSTs. At 25 °C, SWCAs of the complex surfaces increased from 18.2 ± 1.3° to 64.4 ± 1.6° upon increasing the adenine content from 0 to 80%. This behavior can be explained by considering that the hydrophilic groups of adenine and PNIPAAm interacted through NLHB to expose predominantly the hydrophobic groups on the surface [31,32]. When we switched the temperature from 25 °C to 45 °C, the PNIPAAm–adenine complexes retained their thermoresponsive behavior [30], but the difference between the SWCAs at 25 °C and 45 °C decreased upon

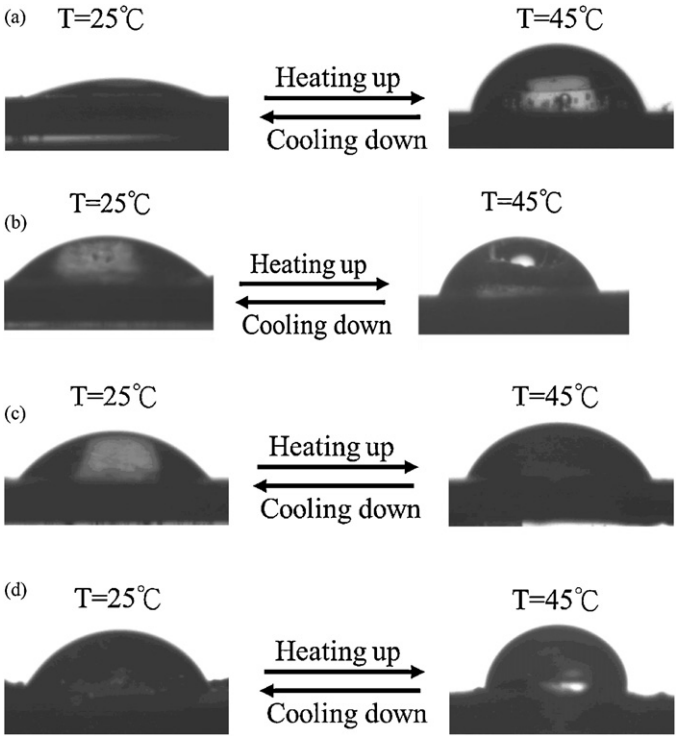

Fig. 4. SWCA images of the surfaces of (a) PNIPAAm, (b) P80A20, (c) P50A50, and (d) P20A80 upon varying the temperature from 25 (left) to 45 °C (right).

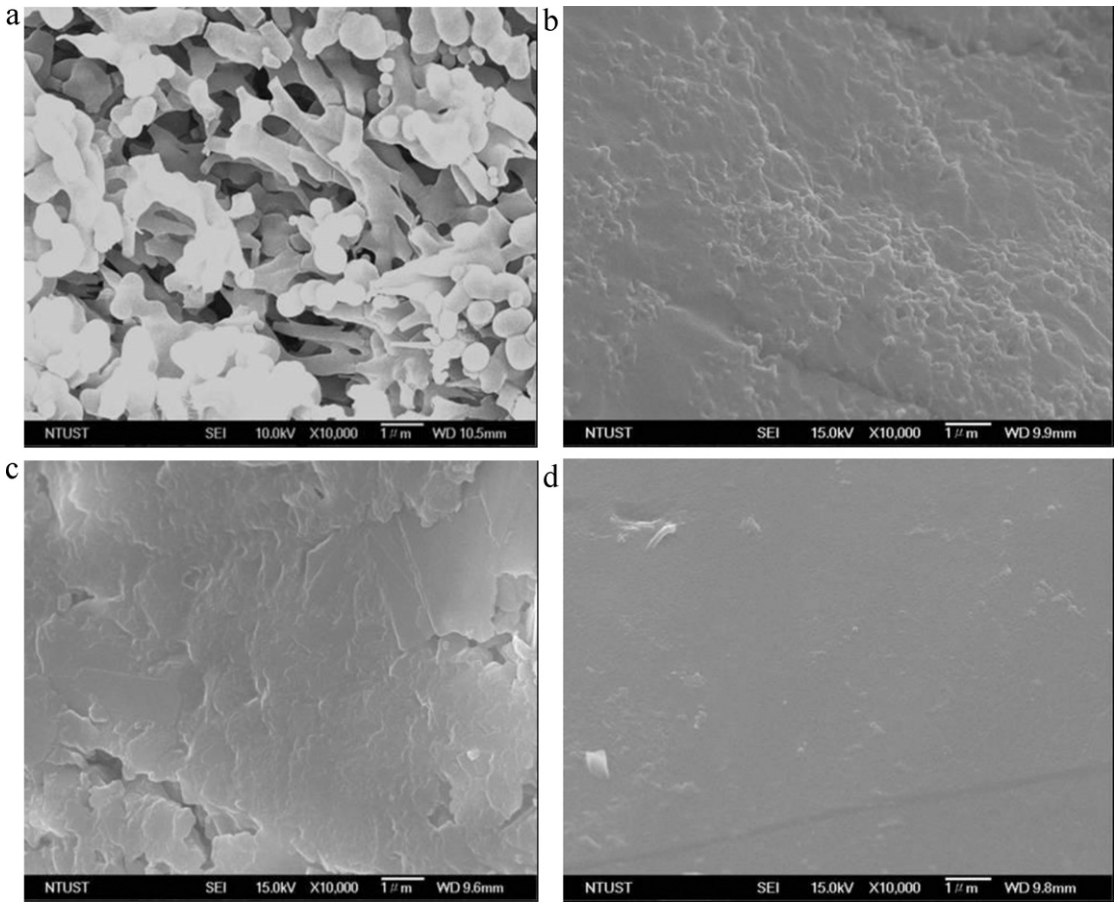

Fig. 5. SEM micrographs of the surfaces of (a) PNIPAAm, (b) P80A20, (c) P50A50, and (d) P20A80.

increasing the adenine content, consistent with a change in the degree of NLHB in the complexes during the phase transition.

Fig. 5 presents FE-SEM images of PNIPAAm and the PNIPAAm–adenine complexes P80A20, P5050, and P20A80. These samples were prepared under the same conditions so that we could assess the reversibility of adenine complexation and its effects on the morphologies of the complexes. Pure PNIPAAm exhibited an irregular microsphere- and wicker-like structure with feature sizes ranging from 200 nm to 1 μm (Fig. 5a). A thin film structure with cracks on the surface appeared instead of the microsphere- and wicker-like structure with increasing the adenine content to 20 wt% for P80A20.(Fig. 5b) Upon increasing the adenine content to 50 wt% (Fig. 5c), the surface achieved a stratum-like texture with interlaced ridges. For P20A80, the stratum-like structures on the surface completely disappeared, revealing a flat surface (Fig. 5d). The surfaces of the complex films without substantial flattening were highly dense and homogeneous when the adenine content increased to 80 wt% [33]. Consequently, NLHB could assist the conformational rearrangement of the PNIPAAm backbone displayed in Scheme 1. Our results suggest that NLHB significantly changed the surface morphology, resulting that the PNIPAAm polymer chains transformed from microgels to assembled films.

Fig. 6 presents WAXD spectra of pure PNIPAAm and adenine and of the complexes P80A20, P5050, and P2080. Two diffraction peaks appear at 7.8° and 19.5° in the spectrum of pure PNIPAAm (Fig. 6a). In addition, the WAXD pattern of pure adenine displays two reflection peaks at 13.6° (d = 0.65 nm) and 27.9° (Fig. 6e); the latter reflection peak corresponds to a d spacing of 0.32 nm, consistent with adenine units undergoing π–π stacking [34], which generally occurs only in a stabilized sheet structure. The WAXS spectrum of the complex P80A20 displays a combination of the features of PNIPAAm and adenine, but a new slight peak at 24° (d = 0.37 nm) implied that intermolecular interactions occurred between PNIPAAm and adenine (Fig. 6b). Upon increasing the adenine content to 50 wt%, the intensity of the diffraction peaks of pure PNIPAAm weakened (Fig. 6c), while that of the crystalline feature peak at 24° increased strongly, indicating that the crystalline structure in the complex was gradually stabilized through NLHB.[35] At adenine

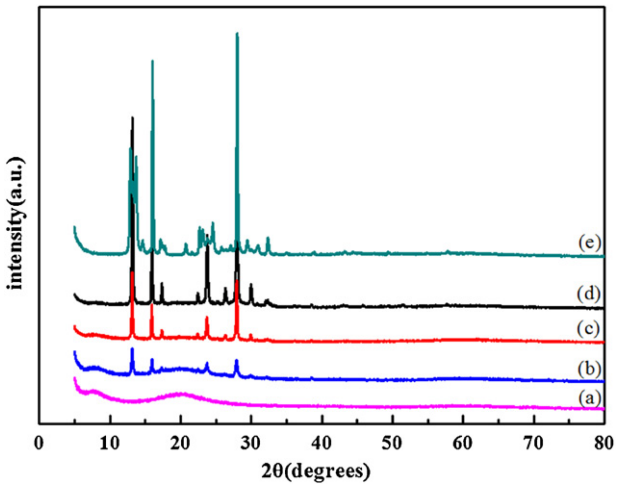

Fig. 6. WAXS data for (a) pure PNIPAAm, (b)P80A20, (c) P50A50, (d) P20A80, and (e) pure adenine.

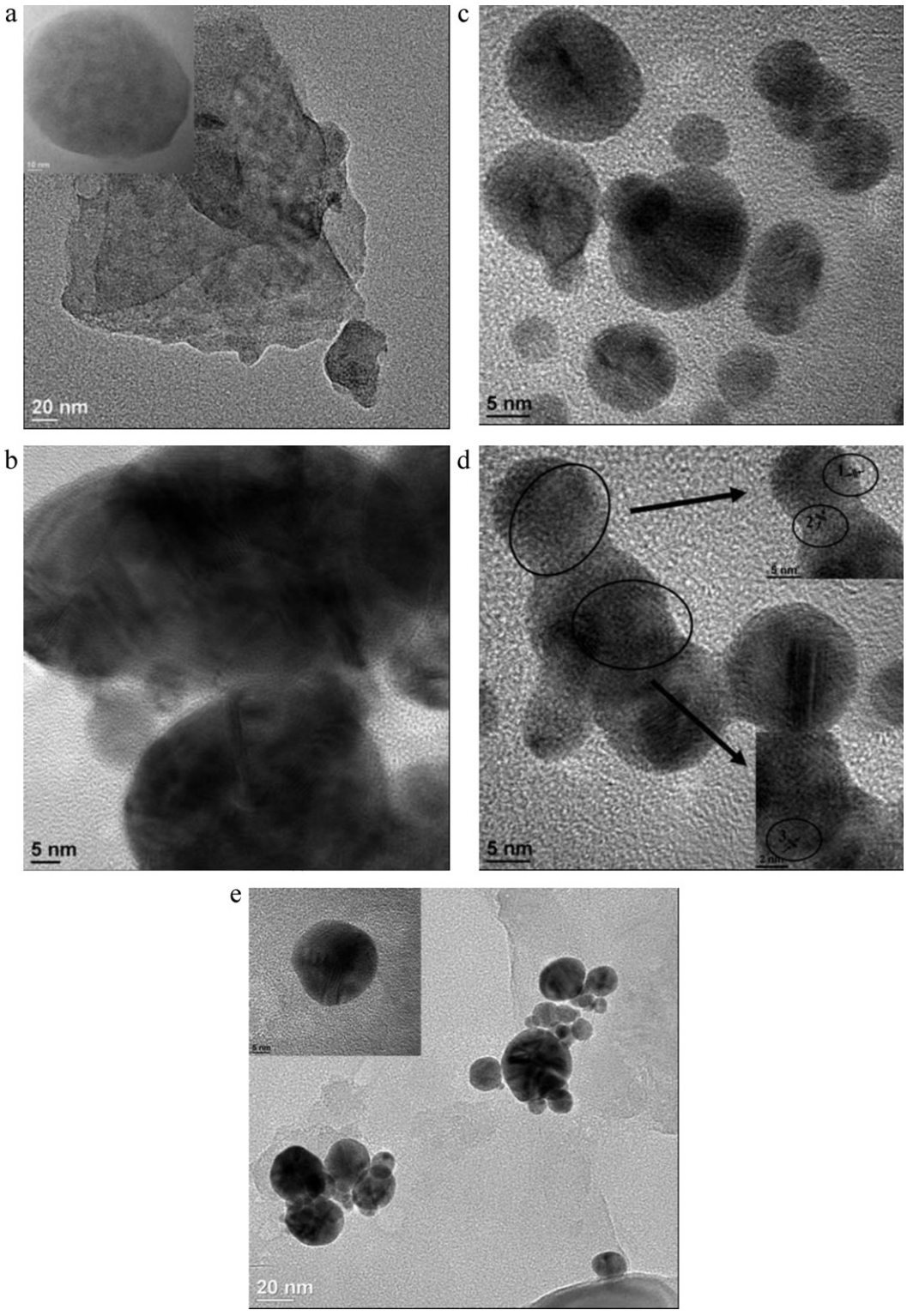

Fig. 7. TEM images of (a) pure PNIPAAm, (b) P80A20, (c) P50A50, (d) P20A80, and (e) pure adenine.

contents above 50 wt%, the adenine units associated the PNIPAAm chains into a apparent crystalline structure. Compared with the peaks of pure adenine, the WAXS spectrum of the P20A80 (Fig. 6d) featured sharper peaks (i.e., it lacked the noise signals of pure adenine), suggesting the rearrangement of the PNIPAAm and adenine in the complexes to a crystalline structure [36].

Fig. 7 displays high-resolution TEM images of pure PNIPAAm, adenine and the complexes P80A20, P50A50, and P20A80. Pure PNIPAAm did not possess an apparent crystalline lattice (Fig. 7a). Upon increasing the adenine content, the lattices of the crystalline complexes appeared clearly (Fig. 7b and c). The optimal lattice of the crystalline complexes occurred for P20A80 (Fig. 7d); even the lattice in the adnine could not be observed with such clarity (Fig. 7e), consistent with the WXRD results. The lattice fringe of a crystalline feature having a regular *d* spacing of 0.37 nm is marked with a descriptor "3" in Fig. 7d; this distance is consistent with the

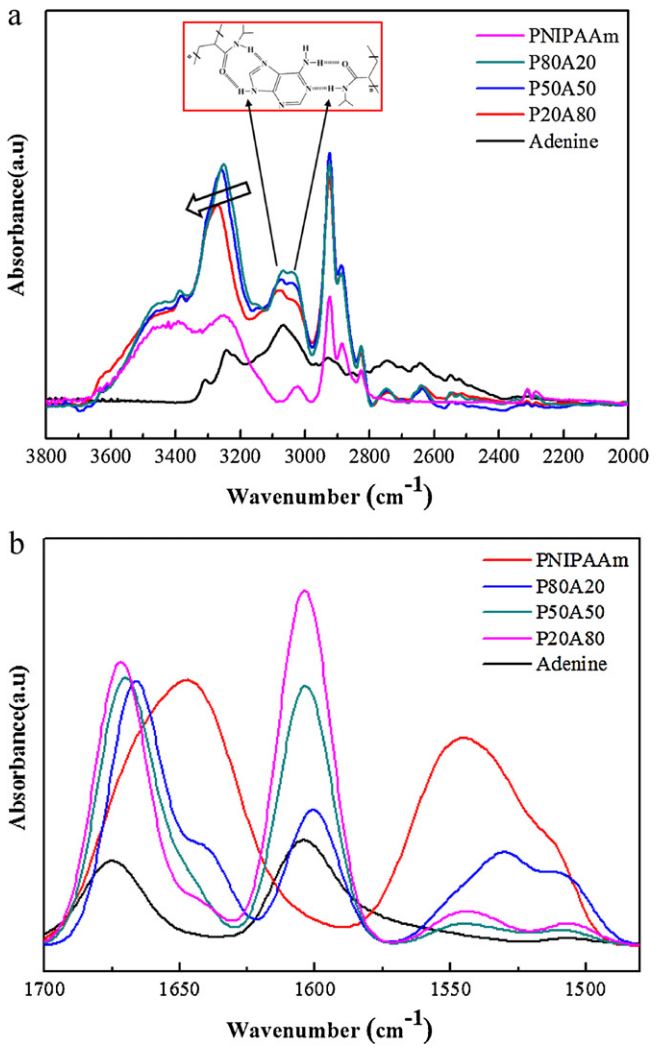

Fig. 8. FTIR spectra [(a) N—H and (b) C=O stretching band regions] of PNIPAAm, adenine, and the PNIPAAm–adenine complexes P80A20, P50A50, and P20A80, recorded at room temperature.

interplanar distance in the P20A80. We also observed some crystalline features possessing lattice fringe distances of 0.65 and 0.32 nm, marked as "1" and "2," respectively, in Fig. 7d, more apparent than the interplanar spacings of crystalline adenine (Fig. 7e) [37].

7.1. FTIR spectroscopic analyses of NLHBs in the complexes

FTIR spectroscopy has been successfully applied in the complexes possessing intermolecular interaction through HB. The NH and OH stretching ranges in a FTIR spectrum are sensitive to the degrees of intermolecular interaction. Fig. 8a displays the film of neat PNIPAAm, two bands appeared near 3269 and 2973 cm^{-1}, attributable to N—H stretching of the amide groups and C—H stretching of sp^3-hybridized carbon atoms. Adenine clear shift of the signal for PNIPAAm at 3269 cm^{-1} occurred in the spectra of the complexes, indicating the disruption of the HBs of PNIPAAm. This peak shifted from 3269 cm^{-1} to 3289 cm^{-1} upon increasing the adenine content to 80 wt%. In addition, the absorption peaks of adenine and PNIPAAm at 3072 and 3021 cm^{-1}, respectively, combined to form a broad peak near 3098 cm^{-1}. We curve-fitted this region of the spectra, resolving the signals into two bands using a least-squares fitting procedure. We assign the bands near 3072 and 3269 cm^{-1} to the NH units involved in NLHB between PNIPAAm and adenine, because of their apparent shift in absorption at room temperature. When adenine became associated with the PNIPAAm main chain, the absorptions of both PNIPAAm and adenine shifted to higher wavenumber (near 3269 cm^{-1}). These result indicate that the free amide N—H decreased on increasing the amount of added adenine, indicating that PNIPAAm associated strongly with adenine, and that PNIPAAm–adenine interactions were more favorable than adenine–adenine interactions[38]. Therefore, the broad signal of the hydrogen-bonded NH groups shifted to higher frequency upon increasing the adenine content, suggesting a switch from strong intramolecular N—H···N—H (PNIPAAm/PNIPAAm) HBs into weak intermolecular N—H···C=O (PNIPAAm/adenine) HBs [39]. Fig. 8b presents FTIR spectra recorded at room temperature to obtain information regarding the NLHB structures of the complexes P80A20, P50A50, and P20A80. The C=O stretching (1659 cm^{-1}) and the CNH vibration (1540 cm^{-1}) of the secondary amide groups also appeared (Fig. 8b) [40]. For adenine, absorption bands appeared at 1673 [σ(N—H)], and 1602 [σ(C=N)] cm^{-1}. We assign the signals at 1607, 1644, and 1669 cm^{-1} to the intermolecularly (sheet structure) and intramolecularly (globule structure) C=O···H—N hydrogen-bonded and free C=O groups (random coil), respectively [39]. The signals of the complexes at 1607 and 1669 cm^{-1} shifted to lower and higher wavenumbers, respectively, upon decreasing the adenine content. These results indicate that the NLHB in the complexes influenced the C=O stretching through intermolecular C=O···H—N HBs as a result of the contributions arising from the different environments surrounding the C=O groups when the amide proton in the free NH group is exchanged [41].

7.2. Quantitative analysis of the NLHB

FTIR spectra of the complexes have received considerable attention because they reveal changes in the conformation, and interactions of the individual chemical groups during its coil-to-globule transition. Fig. 9 displays scale-expanded FTIR spectra of pure PNIPAAm, P80A20, P50A50, P20A80, and adenine in the region from 1500 cm^{-1} to 1700 cm^{-1}, recorded at 30, 60, 120, and 180 °C. In this spectral region, we assign the dominant bands for PNIPAAm at 1646 and 1540 cm^{-1} to amide I and amide II vibrations, respectively. The main contribution to the amide I band is the C=O stretching mode; the amide II band represents mainly in-plane N—H bending.[39] Spectral deconvolution of the amide I band revealed the presence of three components at 1607, 1644, and 1669 cm^{-1}, which we assign to intermolecularly (sheet structure) and intramolecularly (globule structure) hydrogen-bonded and free (or freer) (random coil) C=O groups, respectively, with the majority involved in intramolecular interactions. Similarly, for the amide II band, hydrogen-bonded N—H groups were responsible for the components at 1529 and 1548 cm^{-1} (intra- and inter-molecularly, respectively),[29] with similar relative intensities, with a signal for a minority of free (or freer) N—H groups appearing at 1509 cm^{-1}. The fraction of hydrogen-bonded N—H groups in the amide II band and the fraction of the freer ones and of those involved in intermolecular bonds decreased slightly upon increasing the temperature. For the complexes, all of the signals for the C=O components in the amide I band shifted to lower wavenumbers upon increasing the temperature, indicating that all the intermolecular HBs had been replaced by stronger ones (Fig. 9). Upon increasing the temperature to 180 °C, the component attributed to intramolecularly hydrogen-bonded NH groups appeared near 1644 cm^{-1} for both pure PNIPAAm (Fig. 9a) and P80A20 (Fig. 9b). This signal was due to the coil-to-globule transition from intermolecularly to intramolecularly hydrogen-bonded NH units. This component disappeared partially, however, during the heating of P50A50 and P20A80 (Fig. 9c and d, respectively), implying that the adenine units suppressed the thermal behavior

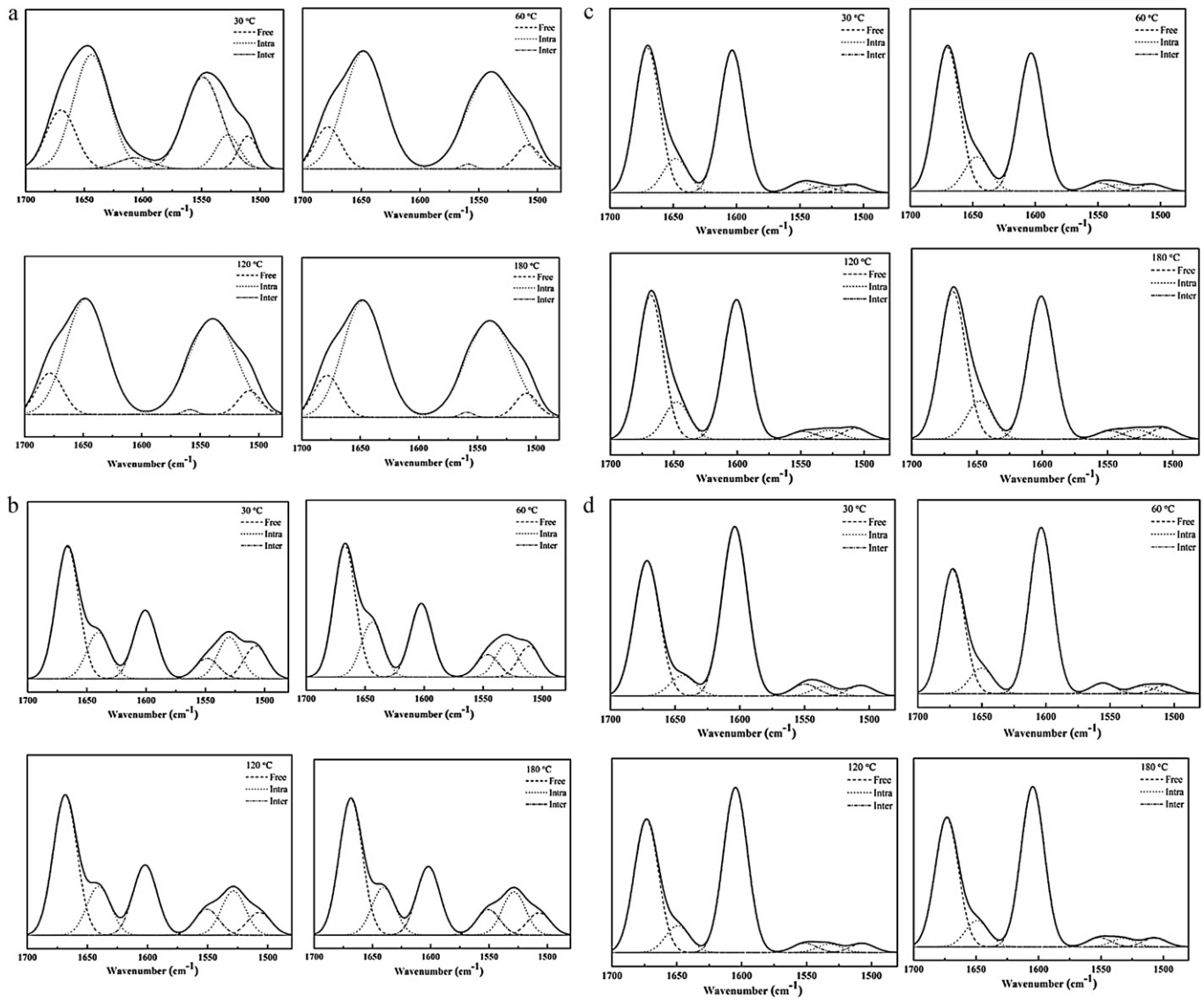

Fig. 9. FTIR spectra (C=O stretching band region) of (a) PNIPAAm, (b) P80A20, (c) P50A50, and (d) P20A80, recorded at 30, 60, 120, and 180 °C.

Table 1
Deconvolution data (positions and relative areas of the components) obtained for relevant regions in the FTIR spectra of pure PNIPAAm, pure adenine, and PNIPAAm–adenine complexes prepared at 30, 60, 120, and 180 °C.

Wavenumber[a], cm^{-1} (area %)						
Assignments	δNH free	δNH intra HB	δNH inter HB	νC=O inter HB[b]	νC=O intra HB[c]	νC=O free[d]
PNIPAAm						
30 °C	1509 (5.5)	1529 (7.2)	1548 (30.6)	1607 (3.4)	1644 (37.4)	1669 (15.6)
60 °C	1507 (4.9)	1539 (41.3)	1558 (0.4)	1600 (0.1)	1647 (43.1)	1678 (9.8)
120 °C	1507 (4.9)	1539 (41.3)	1558 (0.4)	1600 (0.1)	1647 (43.1)	1678 (9.8)
180 °C	1507 (4.9)	1539 (41.3)	1558 (0.4)	1600 (0.1)	1647 (43.1)	1678 (9.8)
PNIPAAm–adenine complexes						
30 °C, P80A20	1507 (9.1)	1529 (7.8)	1548 (8.1)	1600 (20.0)	1640 (16.5)	1666 (38.5)
30 °C, P50A50	1507 (0.3)	1531 (1.8)	1548 (7.2)	1603 (43.8)	1648 (10.2)	1670 (36.7)
30 °C, P20A80	1505 (2.9)	1529 (2.2)	1561 (3.3)	1603 (48.5)	1656 (5.3)	1673 (37.8)
60 °C, P80A20	1510 (8.8)	1529 (9.8)	1549 (6.4)	1602 (19.3)	1644 (17.9)	1667 (37.8)
60 °C, P50A50	1507 (2.6)	1532 (2.1)	1548 (2.4)	1603 (38.8)	1646 (11.7)	1670 (42.4)
60 °C, P20A80	1506 (2.4)	1532 (2.4)	1551 (3.1)	1604 (47.5)	1649 (8.5)	1673 (36.1)
120 °C, P80A20	1505 (6.4)	1527 (14.4)	1548 (5.6)	1602 (14.7)	1641 (19.8)	1668 (39.1)
120 °C, P50A50	1503 (3.1)	1529 (2.6)	1550 (2.2)	1600 (36.9)	1642 (14.2)	1667 (41.0)
120 °C, P20A80	1506 (2.5)	1524 (2.2)	1555 (2.6)	1603 (46.9)	1650 (8.2)	1672 (37.6)
180 °C, P80A20	1505 (6.4)	1527 (14.4)	1548 (5.6)	1602 (14.7)	1641 (19.8)	1668 (39.1)
180 °C, P50A50	1503 (3.1)	1529 (2.6)	1550 (2.2)	1600 (36.9)	1642 (14.2)	1667 (41.0)
180 °C, P20A80	1506 (2.5)	1524 (2.2)	1555 (2.6)	1603 (46.9)	1650 (8.2)	1672 (37.6)

[a] Peak wavenumber.
[b] Inter HB: intermolecular hydrogen bonded (sheet structure).
[c] Intra HB: intramolecular hydrogen bonded (globule structure).
[d] Free: non-hydrogen bonded (random coil).

of PNIPAAm. In addition, the components at 1607 and 1669 cm^{-1} both shifted to higher wavenumbers upon increase of temperature, indicating that the C=O stretching and intermolecularly hydrogen-bonded C=O···H–N bands in the NLHB complexes were weakened through thermal disruption [40].

To quantify the effect of NLHB on the compositions of the individual elemental C=O···H–N stretching vibration bands near 1607, 1644, and 1669 cm^{-1} (assigned to intermolecularly and intramolecularly C=O···H–N hydrogen-bonded and free C=O groups, respectively), we employed a curve-fitting procedure to decompose the spectra in the C=O stretching region into elemental vibrational bands. We calculated the fractions of free and intermolecularly and intramolecularly hydrogen bonded species, designated f_{free}, f_{intra}, and f_{inter}, respectively, on the basis of the Lambert–Beer law:

$$fk = \frac{(Ak/\varepsilon k)}{\sum_{k}(Ak/\varepsilon k)}$$

where A_k and ε_k are the absorbance and absorption coefficient of the elemental spectrum (k = free, intra, or inter).[42] To obtain the fraction of hydrogen-bonded C=O groups, we required the absorptivity ratio for hydrogen-bonded and free C=O groups. Table 1 summarizes the proposed band assignments and deconvolution data, as well as the relative contributions of each component of the bands of pure PNIPAAm and adenine and the complexes. For pure PNIPAAm, the changes in the degrees of intermolecularly and intramolecularly hydrogen-bonded N–H units indicate that the polymer featured predominantly intramolecular HBs upon increasing the temperature from 30 °C to 60 °C. Upon increasing the adenine content in the complexes, the fraction of amide II units decreased gradually, attributable to π–π stacking partially replacing the in-plane N–H. The fractions of amide I bands assigned to intermolecular and intramolecular C=O···H–N hydrogen bonds increased from 20% to 48% and decreased from 16.5% to 5.7% at 30 °C, respectively, upon increasing the adenine content. Intramolecular HB replaced intermolecular HB when the temperature reached 90 °C. Above 120 °C, we observed neither observable changes nor shifts in the components related to the amide II bands. Furthermore, for all the complexes, there were neither observable changes nor shifts in the C–H stretching modes (CH_3 at 2972 cm^{-1}; CH_3 at 2878 cm^{-1}), relative to those in the pure PNIPAAm, suggesting that no hydrophobic interactions occurred between adenine and PNIPAAm.

Fig. 10a and b displays absorption spectra of adenine and the complexes in the visible region at 25 and 45 °C, respectively. Apparent absorptions appeared for the complexes in the UV region, mainly contributed by the adenine units. The absorptions varied with the adenine concentration in the complexes, due to rapid exchange between the associated and dissociated PNIPAAm–adenine complexes. The band was affected in two ways: a decrease in absorbance (hypochromic effect) and a slight shift toward lower wavelength (hypsochromic effect). These effects are all consistent with interactions occurring between PNIPAAm and adenine [43]. Fig. 10c presents a plot of the reciprocal of the concentration of adenine and the change in absorbance at 235 nm according to Eq. (3), both below and above the LCST (at 25 and 45 °C, respectively). We obtained the value of K_a from the slope in this line [44]. Moreover, we observed evidence for temperature-sensitive affinity from a comparison of the plots recorded at 25 and 45 °C, with the values of K_a decreasing abruptly from 4.75×10^4 M^{-1} to 2.78×10^4 M^{-1} upon increasing the temperature from 25 °C to 45 °C, during which PNIPAAm undergoes a coil–globule transition. The higher inter-association equilibrium constant (K_a) of the complex at 25 °C than at 45 °C suggests that the NLHB between

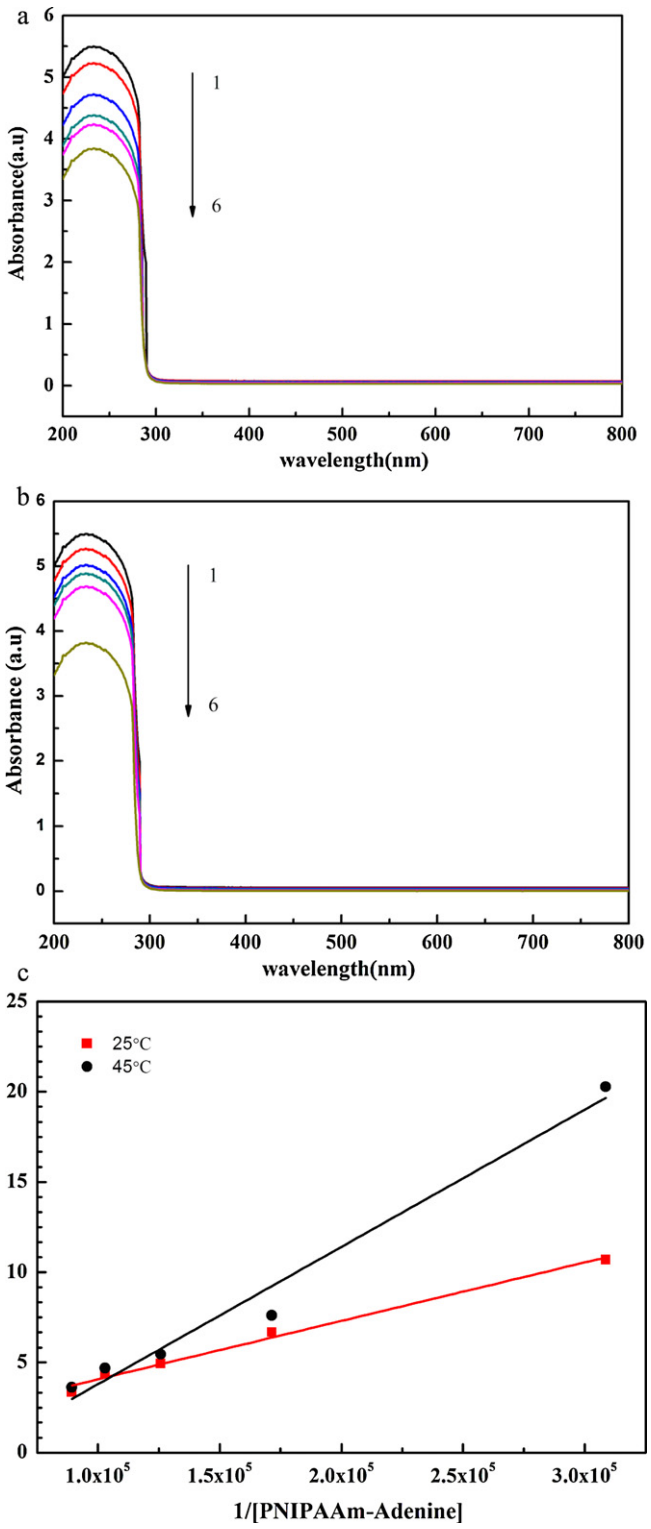

Fig. 10. UV–vis absorption spectra of PNIPAAm–adenine complexes in aqueous solution at (a) 25 and (b) 45 °C. Line 1 represents the spectrum of pure adenine in aqueous solution; lines 2–6 represent concentrations of adenine of 2×10^{-4}, 1×10^{-4}, 1×10^{-3}, and 2×10^{-3} M in aqueous solutions of PNIPAAm (final concentration of PNIPAAm: 1 mg/mL). (c) Double-reciprocal plots of ΔA with respect to [PNIPAAm/adenine] at 25 and 45 °C, according to the linearized formula $\left[\frac{1}{\Delta A} = \frac{1}{K_b A_{max}} \times \frac{1}{[\text{PNIPAAm}]} + \frac{1}{\Delta A_{max}}\right]$.

adenine and PNIPAAm was tunable thermodynamically. The different K_a of the complex at 25 and 45 °C implied the reversibility of complexation and decomplexation of the PNIPAAm and adenine, verifying the DNA capturing-releasing mechanism in our previous reports [10,17,22]. Although a DNA sequence composed of adenine, thymine, guanine and cytosine base pairs is much longer than an adenine unit, the further development of DNA recognition can base on the fundamental mechanism of NLHB interaction between a single base pair and PNIPAAm.

8. Conclusions

We have found the specific interaction between PNIPAAM and adenine, so called NLHB, to generate noncovalently interacting colloidal supramolecule through self-assembly strategy. The complexation of adenine with PNIPAAm hydrogels is a thermodynamically favorable process that can be exploited to tune the thermoresponsive behavior of PNIPAAm, depending on the initial amount of adenine. Adenine as a bioactive HB donor or acceptor for neutrally charged responsive polymers can form complexes, which have potential for understanding the interaction between natural and artificial macromolecules of interest. The strategy of generation specific interaction such NLHB for the fundamental mechanism could be applied widely to recognize the DNA sequence or thermodynamically controlled DNA release formulations using PNIPAAm as a medium with biocompatibility.

Acknowledgment

We thank the National Science Council of the Republic of China for supporting this research financially.

References

[1] P.S. Stayton, T. Shimoboji, C. Long, A. Chilkoti, G.H. Chen, J.M. Harris, A.S. Hoffman, Nature 378 (1995) 472–474.
[2] J.K. Chen, C.H. Chan, F.C. Chang, Applied Physics Letters 92 (2008) 053108.
[3] C.H. Chan, J.K. Chen, F.C. Chang, Sensors and Actuators B 13 (2008) 327–332.
[4] Y. Osada, H. Okuzaki, H. Hori, Nature 355 (1992) 242–244.
[5] J.-K. Chen, B.-J. Bai, F.-C. Chang, Applied Physics Letter 99 (2011) 013701.
[6] J.-K. Chen, B.-J. Bai, Sensors and Actuators B 160 (2011) 1011–1019.
[7] J.K. Chen, A.-L. Zhuang, Journal of Physical Chemistry C 114 (2010) 11801–11809.
[8] J.K. Chen, C.Y. Hsieh, C.F. Huang, P.M. Li, S.W. Kuo, F.C. Chang, Macromolecules 41 (2008) 8729–8736.
[9] M. Taha, B.S. Gupta, I. Khoiroh, M.J. Lee, Macromolecules 44 (2011) 8575–8589.
[10] J.-K. Chen, J-Y. Li, Journal of Colloid and Interface Science 358 (2011) 454–461.
[11] A.C. Lima, W. Song, B. Blanco-Fernandez, C. Alvarez-Lorenzo, J.F. Mana, Pharmaceutical Research 28 (2011) 1294–1305.
[12] H.F. Lu, E.D. Targonsky, M.B. Wheeler, Y.L. Cheng, Biotechnology and Bioengineering 96 (2007) 146–155.
[13] M.E. Nash, W.M. Carroll, R.Y. Nikoloskya, C.O. Commell, A.V. Gorelov, P. Dockery, C. Liptrot, F.M. Lyng, A. Garcia, Y.A. Rochev, ACS Applied Materials & Interfaces 6 (2011) 1980–1990.
[14] R.G. Shaikh, S.V. Shah, K.N. Patel, B.A. Patel, P.A. Patel, International Journal for Pharmaceutical Research Scholars (2012) 17–34.
[15] E.S. Gil, S.M. Hudson, Progress in Polymer Science 29 (2004) 1173–1222.
[16] J.-K. Chen, J.-Y. Li, Applied Physics Letter 97 (2010) 063701.
[17] K. Ariga, T. Kunitake, Accounts of Chemical Research 31 (1998) 1–378.
[18] L.V. Yakushevich, S. Gapa, J. Awrejcewicz, International Journal of Bifurcation and Chaos 21 (10) (2011) 3063–3071.
[19] C. McHugh, C. Erxleben, Crystal Growth & Design 11 (2011) 5096–5104.
[20] D. Wang, Y. Su, C. Jin, B. Zhu, Y. Pang, L. Zhu, J. Liu, C. Tu, D. Yan, X. Zhu, Biomacromolecules 12 (2011) 1370–1379.
[21] Y. Sato, O. Niwa, F. Mizutani, Sensors and Actuators B: Chemical 121 (2007) 214–218.
[22] J.-K. Chen, J.-Y. Li, Sensors and Actuators B 150 (2010) 314–320.
[23] D. Xiong, Z. Li, R. Ma, Y. An, L. Shi, Journal of Polymer Science Part A: Polymer Chemistry 47 (2009) 1651–1660.
[24] J.-K. Chen, J.-H. Wang, S.-K. Fan, J.-Y. Chang, The Journal of Physical Chemistry C 116 (2012) 6980–6992.
[25] Y.Y. Liu, X.D. Fan, Y.b. Zhao, Journal of Polymer Science: Part A: Polymer Chemistry 43 (2005) 3516–3524.
[26] I.D. Kuntz Jr., F.P. Gasparro, M.D. Johnston Jr., R.P. Taylor, Journal of the American Chemical Society 90 (1968) 4778–4781.
[27] B.S. Tian, C. Yang, The Journal of Physical Chemistry C 113 (2009) 4925–4931.
[28] Z.X. Zhang, K.L. Liu, J. Li, Macromolecules 44 (2011) 1182–1193.
[29] S.Y. Lin, K.S. Chen, L.R. Chu, Polymer 40 (1999) 2616–2624.
[30] Q. Yu, Y. Zhang, H. Chen, F. Zhou, Z. Wu, H. Huang, J.L. Brash, Langmuir 26 (2010) 8582–8588.
[31] L. Chen, M. Liu, H. Bai, P. Chen, F. Xia, D. Han, L. Jiang, Journal of the American Chemical Society 131 (2009) 10467–10472.
[32] T.-Y. Chen, J.-K. Chen, Colloid and Polymer Science 289 (2011) 433–445.
[33] Y. Lu, Y.J. Choi, H.S. Lim, D. Kwak, C. Shim, S.G. Lee, K. Cho, Langmuir 26 (2010) 17749–17755.
[34] C.C. Cheng, Y.C. Yen, Y.S. Ye, F.C. Chang, Journal of Polymer Science, Part A: Polymer Chemistry 47 (2009) 6388–6395.
[35] S.Y. Kim, S.M. Cho, Y.M. Lee, S.J. Kim, Journal of Applied Polymer Science 78 (2000) 1381–1391.
[36] A. Dawn, A.K. Nandi, Macromolecular Bioscience 5 (2005) 441–450.
[37] J.-J. Wu, T.-R. Lu, C.-T. Wu, T.-Y. Wang, L.-C. Chen, K.-H. Chen, C.-T. Kuo, T.-M. Chen, Y.-C. Yu, C.-W. Wang, E.-K. Lin, Diamond and Related Materials 8 (1999) 605–609.
[38] H.H. Hammuda, G. Nemer, W. Sawma, J. Touma, P. Barnabe, Y. Bou-Mouglabey, A. Ghannoum, J. El-Hajjar, J. Usta, Chemico-Biological Interactions 173 (2008) 84–96.
[39] E. Costa, M. Coelho, L.M. Ilharco, A. Aguiar-Ricardo, P.T. Hammond, Macromolecules 44 (2011) 612–621.
[40] S.Y. Yang, M.F. Rubner, Journal of the American Chemical Society 124 (2002) 2100–2101.
[41] Y. Katsumoto, T. Tanaka, K. Ihara, M. Koyama, Y. Ozaki, Journal of Physical Chemistry B 111 (2007) 12730–12737.
[42] L. Guo, H. Sato, T. Hashimoto, Y. Ozaki, Macromolecules 43 (2010) 3897–3902.
[43] N.K. Janjua, A. Siddiqa, A. Yaqub, S. Sabahat, R. Qureshi, S.U. Haque, Spectrochimica Acta Part A: Molecular and Biomolecular Spectroscopy 74 (2009) 1135–1137.
[44] L.Z. Zhang, G.Q. Tang, Journal of Photochemistry and Photobiology B: Biology 74 (2004) 119–125.